Am J Physiol Heart Circ Physiol 292: H2654–H2663, 2007.
First published February 7, 2007; doi:10.1152/ajpheart.01255.2006.

Activators of the PKA and PKG pathways attenuate RhoA-mediated suppression of the K_{DR} current in cerebral arteries

Kevin D. Luykenaar and Donald G. Welsh

Department of Physiology and Biophysics, University of Calgary, Alberta, Canada

Submitted 16 November 2006; accepted in final form 30 January 2007

Luykenaar KD, Welsh DG. Activators of the PKA and PKG pathways attenuate RhoA-mediated suppression of the K_{DR} current in cerebral arteries. *Am J Physiol Heart Circ Physiol* 292: H2654–H2663, 2007. First published February 7, 2007; doi:10.1152/ajpheart.01255.2006.—This study tested whether activation of protein kinase A (PKA) and G (PKG) pathways would attenuate the ability of RhoA to suppress the delayed rectifier K^+ (K_{DR}) current and limit agonist-induced depolarization and constriction. Smooth muscle cells from rat cerebral arteries were enzymatically isolated, and whole cell K_{DR} currents were monitored with conventional patch-clamp electrophysiology. The K_{DR} current averaged 21.2 ± 2.3 pA/pF (mean ± SE) at +40 mV and was potently inhibited by UTP. Current suppression was eliminated in the presence of C3 exoenzyme, confirming that this modulation is dependent on RhoA. Activation of PKA (dibutyryl-cAMP, forskolin) or PKG (dibutyryl-cGMP, sodium nitroprusside, nitric oxide) similarly abolished the ability of UTP to suppress K_{DR} and did so without effect on baseline current. Using pressure myography techniques, we stripped cerebral arteries of endothelium and preconstricted them with UTP; these were subsequently shown to hyperpolarize and dilate to both forskolin and sodium nitroprusside. An increase in K_V channel activity was found to partly underlie these associated changes, as constriction to 4-aminopyridine (K_{DR} channel blocker) was greater after PKA or PKG activation. We conclude from our electrophysiological and functional observations that the PKA and PKG pathways attenuate the ability of UTP to depolarize and constrict cerebral arteries in part by minimizing the RhoA-mediated suppression of the K_{DR} current.

cyclic nucleotides; pyrimidine nucleotides; Rho signaling; smooth muscle

AN INTEGRATED NETWORK OF RESISTANCE arteries effectively controls blood flow to the cerebral circulation. Under dynamic conditions, arterial tone is regulated by a variety of factors, including metabolism (11), humoral and neural stimuli (28), blood flow (8), and intraluminal pressure (12, 16). Many vasoactive stimuli initiate changes in arterial tone by activating transduction pathways associated with G-protein-coupled receptors. It is key proteins within such pathways that in turn influence the Ca^{2+} sensitivity of the myofilament (29) and/or ion channels that control cytosolic Ca^{2+} through changes in resting membrane potential (E_m) (20).

The Rho pathway is a primary signaling cascade controlling smooth muscle contraction. The key molecular switch within this pathway is RhoA, a small GTPase typically activated by receptors coupled to $G_{12/13}$ and Rho guanine nucleotide exchange factors (4, 25, 30). In the active GTP-bound state, RhoA is targeted to the sarcolemma (10) where it associates with its principal downstream effector, Rho kinase (31). Activated Rho kinase in turns inhibits myosin light-chain phosphatase, increasing the phosphorylation state of myosin and the contractile response to available Ca^{2+} (31). In addition to sensitizing the contractile apparatus, recent studies have indicated that RhoA signaling plays an important role in modulating ion channels (9, 18). This includes the inhibition of the delayed rectifying K^+ (K_{DR}) current, a response that enables agonists such as UTP to depolarize and constrict intact cerebral arteries (18).

Recent investigations have noted that RhoA signaling is strongly influenced by the activity of protein kinase A (PKA) and G (PKG). In particular, these kinases have been reported to phosphorylate active, membrane-bound RhoA and to promote protein translocation to the cytosol (6, 17, 19, 24, 26). Without membrane localization, it is difficult for RhoA to activate downstream effectors such as Rho kinase. Smooth muscle relaxation typically ensues, and most studies have ascribed this functional effect to reduced Ca^{2+} sensitization (19, 24). Although Ca^{2+} sensitization is important, one should not overlook the possibility that PKA and PKG may also promote smooth muscle relaxation by limiting the ability of active RhoA to inhibit K_{DR} channels and depolarize vascular smooth muscle.

In this study, we examined whether the activation of the PKA and PKG pathways would attenuate the ability of RhoA to inhibit K_{DR} channels and to depolarize and constrict intact cerebral arteries. Initial measurements revealed the presence of a K_{DR} current in cerebral arterial smooth muscle cells; this current was potently inhibited by UTP through a RhoA-dependent mechanism. Activators of PKA and PKG impeded the ability of UTP to inhibit the K_{DR} current without affecting baseline channel activity. Functional experiments demonstrated that PKA and PKG activators hyperpolarized and dilated UTP-constricted cerebral arteries, a response that could be partly ascribed to the increased activity of 4-aminopyridine (4-AP)-sensitive K_{DR} channels. In summary, our findings reveal a novel regulatory mechanism in the cerebral circulation, whereby PKA and PKG pathways limit RhoA-dependent suppression of the 4-AP-sensitive K_{DR} current. This mechanism may be essential in preventing agonists from overly constricting cerebral arteries and impairing tissue blood flow.

MATERIALS AND METHODS

Animal procedures and tissue preparation. All animal procedures were approved by the University of Calgary Animal Care and Use Committee. In brief, female Sprague-Dawley rats (10–12 wk of age) were euthanized by carbon dioxide asphyxiation. The brain was

Address for reprint requests and other correspondence: D. G. Welsh, Smooth Muscle Research Group, HMRB-G86, Heritage Medical Research Bldg., Univ. of Calgary, 3330 Hospital Dr. N.W., Calgary, Alberta, Canada, T2N-4N1 (e-mail: dwelsh@ucalgary.ca).

The costs of publication of this article were defrayed in part by the payment of page charges. The article must therefore be hereby marked "*advertisement*" in accordance with 18 U.S.C. Section 1734 solely to indicate this fact.

carefully removed and placed in cold PBS (pH 7.4) solution containing (in mM) 138 NaCl, 3 KCl, 10 Na_2HPO_4, 2 NaH_2PO_4, 5 glucose, 0.1 $CaCl_2$, and 0.1 $MgSO_4$. Middle cerebral arteries were carefully dissected free of connective tissue and cut into ~2-mm segments.

Isolation of arterial smooth muscle cells. Smooth muscle cells from cerebral arteries were enzymatically isolated as previously described (32). Briefly, segments of cerebral arteries were placed in an isolation medium containing (in mM) 60 NaCl, 80 sodium glutamate, 5 KCl, 2 $MgCl_2$, 10 glucose, and 10 HEPES with 1 mg/ml albumin (pH 7.4). After a 10-min equilibration at 37°C, the tissue was incubated for 15 min in the same medium supplemented with 0.5 mg/ml papain and 1.5 mg/ml DTT. This was followed by 10-min incubation in isolation medium containing 100 μM Ca^{2+}, 0.7 mg/ml type F collagenase, and 0.4 mg/ml type H collagenase. After enzyme treatment, the tissue was washed repeatedly in ice-cold isolation medium and triturated with a fire-polished pipette to liberate myocytes. Isolated cells were kept in ice-cold isolation medium for use the same day.

Electrophysiology. Conventional patch-clamp electrophysiology was used to measure whole cell K_{DR} currents in isolated cerebral myocytes as described previously (18). Recording electrodes (resistance of 4–7 MΩ) were fashioned from borosilicate glass, covered in sticky wax to reduce capacitance, and backfilled with pipette solution containing (in mM) 110 potassium gluconate, 30 KCl, 0.5 $MgCl_2$, 5 HEPES, 10 EGTA, 5 Na_2ATP, and 1 GTP (pH 7.2). To attain whole cell configuration, a pipette was lowered onto an isolated smooth muscle cell, and negative pressure was applied to rupture the membrane and achieve a gigaohm seal. Cells were voltage clamped (−60 mV) in a bath solution containing (in mM) 120 NaCl, 3 $NaHCO_3$, 4.2 KCl, 1.2 KH_2PO_4, 2 $MgCl_2$, 0.1 $CaCl_2$, 10 glucose, and 10 HEPES (pH 7.4). A 1 M NaCl-agar salt bridge between the Ag-AgCl reference electrode and the bath solution was used to minimize offset potentials. Liquid junction potentials were measured and were <2 mV. Whole cell currents were recorded on an Axopatch 200B amplifier (Axon Instruments, Union City, CA), filtered at 1 kHz, digitized at 5 kHz, and stored on a computer for subsequent analysis with Clampfit 8.1 software. Cell capacitance was measured with the cancellation circuitry in the voltage-clamp amplifier and averaged at 19.3 ± 0.6 pF. Cells displaying a noticeable (>0.3 pF) shift in capacitance during experiments were excluded from analysis. All experiments were performed at room temperature (20–22°C).

Experimental protocol and isolated smooth muscle cells. Voltage-clamped cells were equilibrated for 15 min before experimentation. Whole cell K_{DR} currents were monitored under control conditions, in the presence of UTP, and in response to increased concentrations of 4-AP. To implicate RhoA in UTP-mediated suppression, C3 exoenzyme was dialyzed into the cell before we measured the effect of UTP. To ascertain the effects of PKA and PKG signaling, myocytes were preincubated in dibutyryl-cAMP (db-cAMP; 2×10^{-4} M), forskolin (1×10^{-6} M), dibutyryl-cGMP (db-cGMP; 1×10^{-4} M), sodium nitroprusside (SNP; 2×10^{-5} M), or nitric oxide before the addition of UTP. In general, the net current-voltage relationship was determined by measuring the peak current at the end of a 300-ms pulse to voltages from −70 to +40 mV. After each pulse, a voltage step to −40 mV was used to monitor tail currents for the assessment of steady-state activation. Tail currents were calculated as the difference between the peak amplitude of the tail and the sustained level of

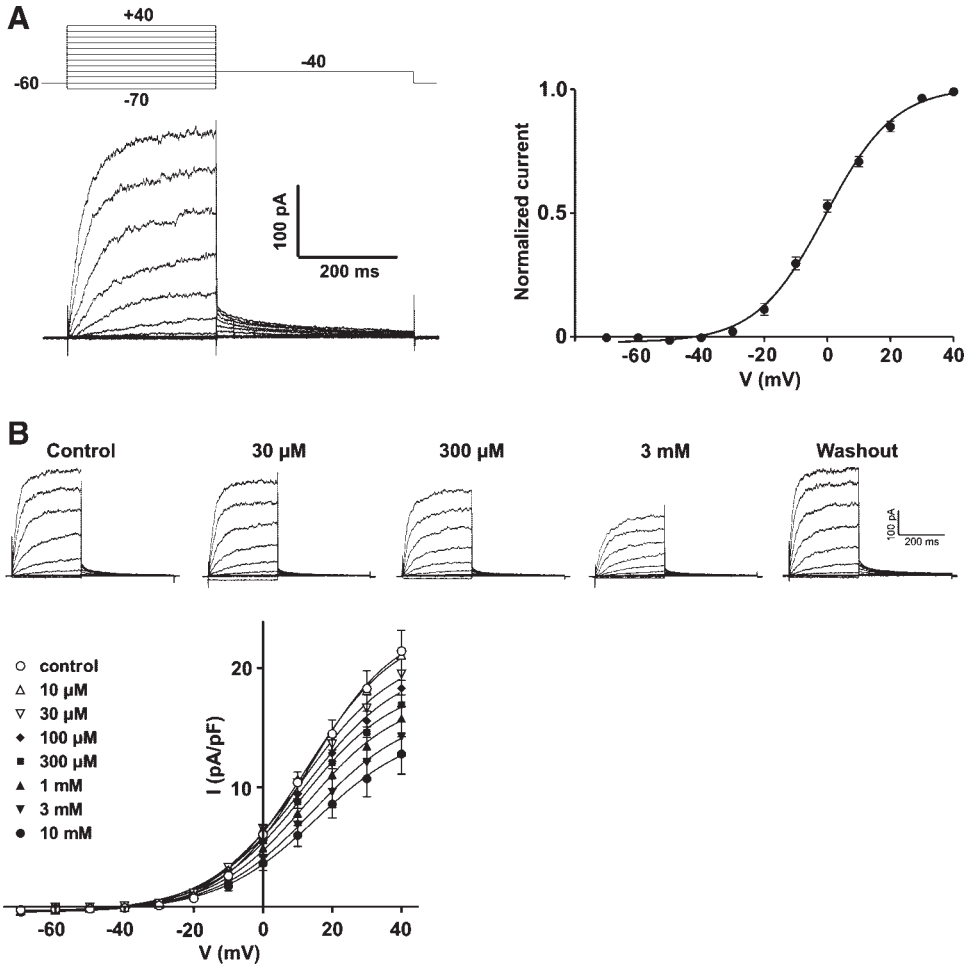

Fig. 1. Delayed rectifier K^+ (K_{DR}) current in myocytes isolated from rat cerebral arteries. *A*: voltage (*V*) paradigms (*top left*) were designed to measure steady-state activation. Representative recording of whole cell K_{DR} current is shown in *bottom left*. *Right*: plot of steady-state activation. Solid line is Boltzmann distribution function with half-maximal activation occurring at −0.56 ± 0.66 mV (n = 12). *B*, *top*: representative recordings of K_{DR} current before and after the addition of increasing concentrations of 4-aminopyridine (4-AP). *B*, *bottom*: net current-voltage (*I–V*) relationship of K_{DR} current under control conditions and in the presence of increasing concentrations of 4-AP (n = 7).

current at −40 mV. Data were fitted to a Boltzmann distribution function to determine the voltage for half-maximal activation.

Intact cerebral arteries. Cerebral artery segments (~2 mm in length) were mounted in a customized arteriograph chamber (J.B. Pierce Laboratory, New Haven, CT) and superfused with warm (37°C) physiological salt solution (pH 7.4) containing (in mM) 119 NaCl, 4.7 KCl, 20 $NaHCO_3$, 1.7 KH_2PO_4, 1.2 $MgSO_4$, 1.6 $CaCl_2$, and 10 glucose. Endothelial cells were removed from all arteries by passing air bubbles through the lumen of the vessel, the success of which was confirmed by the loss of bradykinin-induced dilations. Arteries were maintained under no flow conditions and at low intraluminal pressure (15 mmHg) so that agonist responses could be examined independent of myogenic mechanisms. Arterial diameter was monitored with an automated edge detection system (IonOptix, Milton, MA). Smooth muscle E_m was assessed by inserting a glass microelectrode (tip resistance = 120–150 MΩ) filled with 1 M KCl carefully into the vessel wall and recording the voltage difference across the membrane with an intracellular electrometer (Warner Instruments, Hamden, CT). The criteria for successful cell impalement included *1*) a sharp negative E_m deflection upon entry, *2*) a stable recording for at least 1 min after entry, and *3*) a sharp return to baseline upon electrode removal. Because E_m recordings were typically limited to 3–10 min, a separate impalement was required to measure E_m under each experimental condition.

Experimental protocol and intact cerebral arteries. Cerebral arteries were equilibrated for 60 min at 37°C before experimentation. Contractile ability was assessed by briefly (~10 s) exposing cerebral arteries to a 6×10^{-2} M KCl challenge. Changes in arterial diameter and smooth muscle E_m were measured under control conditions, in response to UTP and in the presence of forskolin (1×10^{-6} M) or SNP (2×10^{-4} M). Constriction to 4-AP (5×10^{-3} M) was also used as a functional index of K_{DR} channel activity in cerebral arteries exposed to UTP alone or in combination with forskolin or SNP.

Chemicals, drugs, and enzymes. Buffer reagents, collagenases (types F and H), UTP, 4-AP, and SNP were obtained from Sigma (St. Louis, MO). Papain was acquired from Worthington (Lakewood, NJ). C3 exoenzyme, db-cAMP, db-cGMP, and forskolin were purchased from Calbiochem (La Jolla, CA). C3 exoenzyme was dissolved in DMSO with a final solvent concentration ≤0.05%. Nitric oxide stock solution (1.9 mM) was made up by saturating deoxygenated ultra-pure water with nitric oxide gas.

Statistical analysis. Data are expressed as means ± SE, and *n* indicates the number of vessels or cells. Paired *t*-tests were performed to statistically compare the effects of a given condition or treatment on arterial diameter, E_m, or whole cell current. If more than two conditions or treatments were being compared, a repeated-measures ANOVA was used. When appropriate, a Tukey-Kramer pairwise comparison was used for post hoc analysis. *P* values ≤0.05 were considered statistically significant.

RESULTS

K_{DR} current in isolated cerebral smooth muscle cells. Using conventional whole cell patch-clamp electrophysiology and a pipette solution that minimizes BK_{Ca} channel activity, we identified the K_{DR} current in smooth muscle cells isolated from rat cerebral arteries. Figure 1*A* shows a typical K_{DR} current where voltage steps positive to −40 mV elicited activation without noticeable inactivation. To examine the voltage dependence of steady-state activation, tail currents (at −40 mV) were monitored before deactivation as an indication of the proportion of channels open after a given test pulse. As evident in the normalized data, activation occurred at voltages positive to −40 mV and was near maximal at +30 mV (Fig. 1*A*, *right*). Fitting the data to a Boltzmann function established a voltage

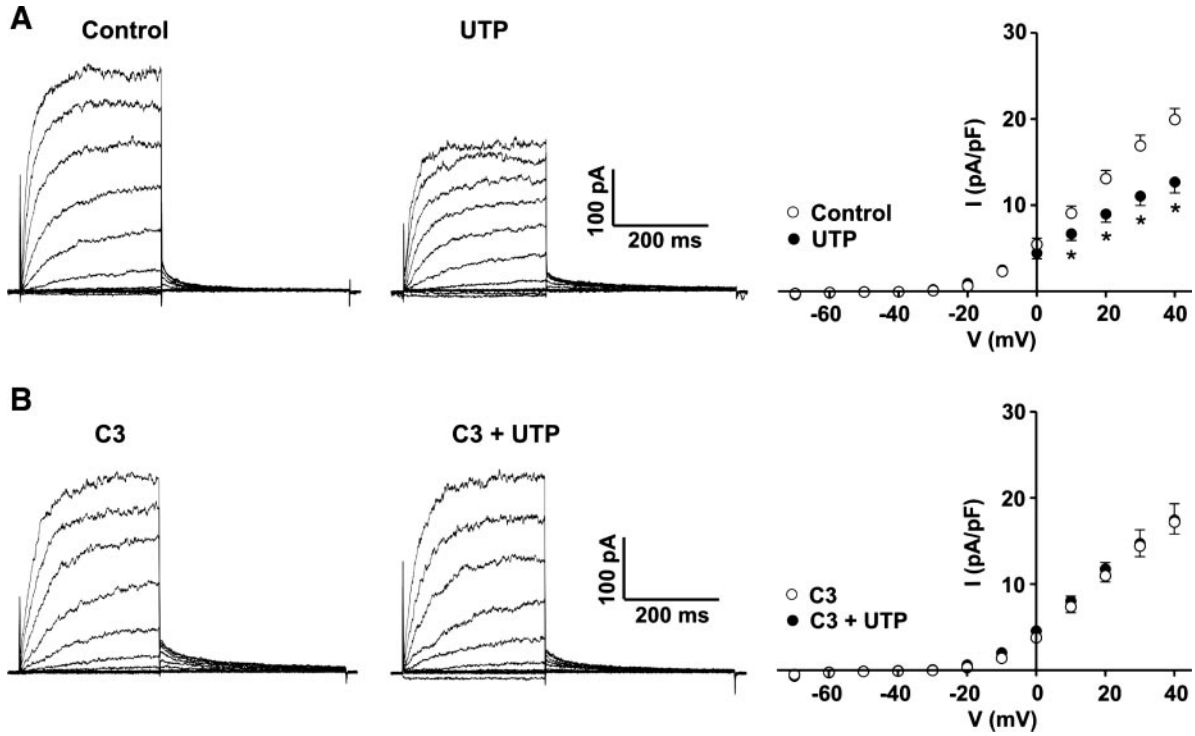

Fig. 2. K_{DR} current suppression by UTP is dependent on RhoA activity. *A*, *left*: representative recordings of K_{DR} current before and after the addition of UTP (3×10^{-5} M). Voltage protocol as in Fig. 1*A*. *A*, *right*: net *I–V* relationship under control conditions and in the presence of UTP ($n = 9$). *B*, *left*: representative recordings demonstrating the effect of UTP (3×10^{-5} M) on K_{DR} current with C3 exoenzyme (C3; 10 mg/ml) and NAD^+ (5×10^{-5} M) in the pipette solution. *B*, *right*: net *I–V* relationship in the presence of C3 + NAD^+ ± UTP ($n = 6$). *Statistical difference ($P \leq 0.05$).

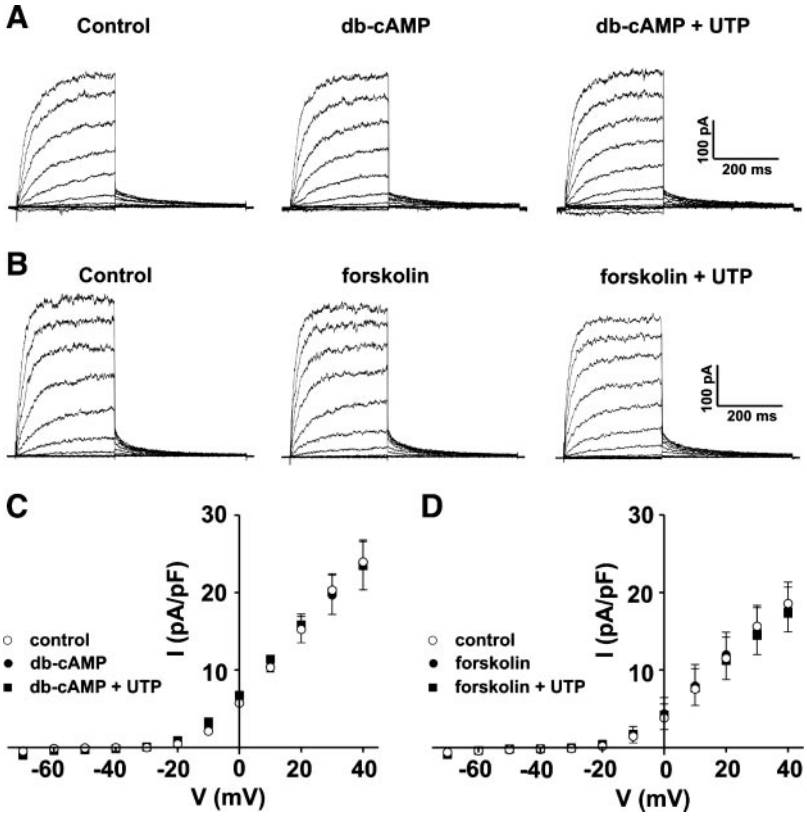

Fig. 3. PKA activation attenuates K_{DR} current suppression by UTP. *A*: representative recordings of K_{DR} current under control conditions and in the presence of 2×10^{-4} M dibutyryl-cAMP (db-cAMP) ± UTP (3×10^{-5} M). *B*: representative recordings of K_{DR} current under control conditions and in the presence of 1×10^{-6} M forskolin ± UTP (3×10^{-5} M). Voltage protocols are as in Fig. 1*A*. *C*: net *I–V* relationship under control conditions and in the presence of db-cAMP ± UTP ($n = 6$). *D*: net *I–V* relationship under control conditions and in the presence of forskolin ± UTP ($n = 6$).

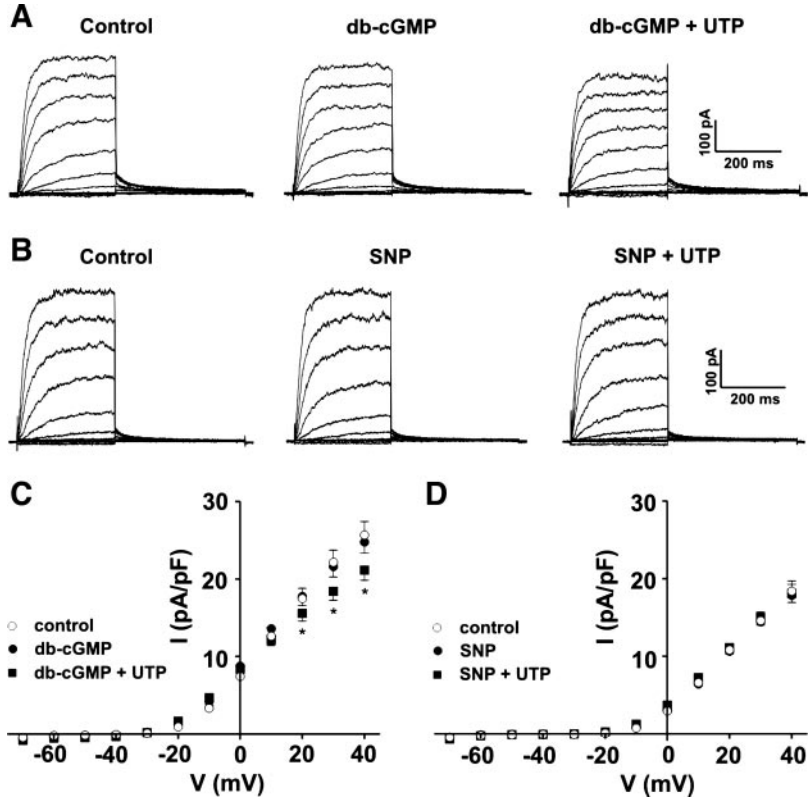

Fig. 4. PKG activation attenuates K_{DR} current suppression by UTP. *A*: representative recordings of K_{DR} current under control conditions and in the presence of 1×10^{-4} M dibutyryl-cGMP (db-cGMP) ± UTP (3×10^{-5} M). *B*: representative recordings of K_{DR} current under control conditions and in the presence of 2×10^{-5} M sodium nitroprusside (SNP) ± UTP (3×10^{-5} M). Voltage protocols are as in Fig. 1*A*. *C*: net *I–V* relationship under control conditions and in the presence of db-cGMP ± UTP ($n = 6$). *D*: net *I–V* relationship under control conditions and in the presence of SNP ± UTP ($n = 6$). *Statistical difference from control ($P \leq 0.05$).

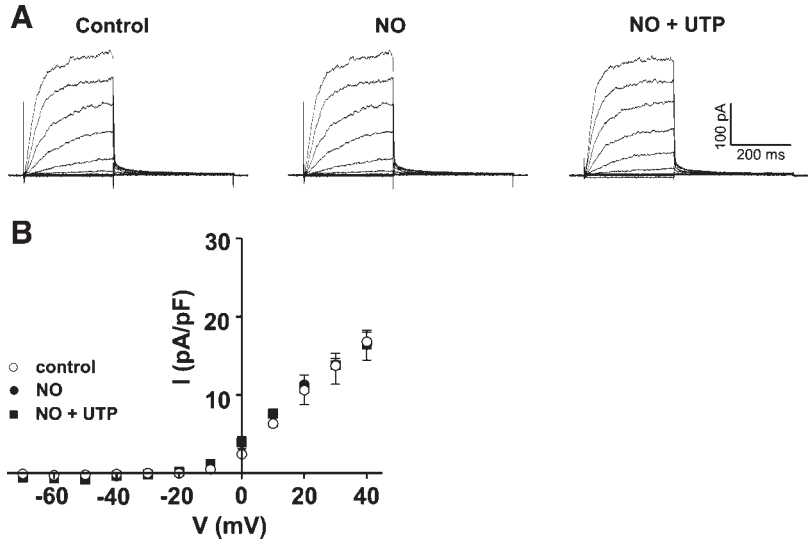

Fig. 5. Guanylate cyclase activation by nitric oxide (NO) attenuates K_{DR} current suppression by UTP. *A*: representative recordings of K_{DR} current under control conditions and in the presence of 1×10^{-7} M NO ± UTP (3×10^{-5} M). Voltage protocols are as in Fig. 1*A*. *B*: net *I–V* relationship under control conditions and in the presence of NO ± UTP ($n = 3$).

for half-maximal activation of −0.56 ± 0.66 mV, consistent with what we have previously found for the cerebral arterial K_{DR} current (18).

The K_{DR} current in cerebral smooth muscle is composed of 4-AP-sensitive and insensitive components (18, 23). We examined 4-AP sensitivity and found the K_{DR} current was reduced in a concentration-dependent manner; this inhibition could be readily washed out (Fig. 1*B*). In general, 4-AP initiated a substantial block at micromolar concentrations (20.7 ± 2.7% with 300 μM 4-AP at +40 mV), with this effect

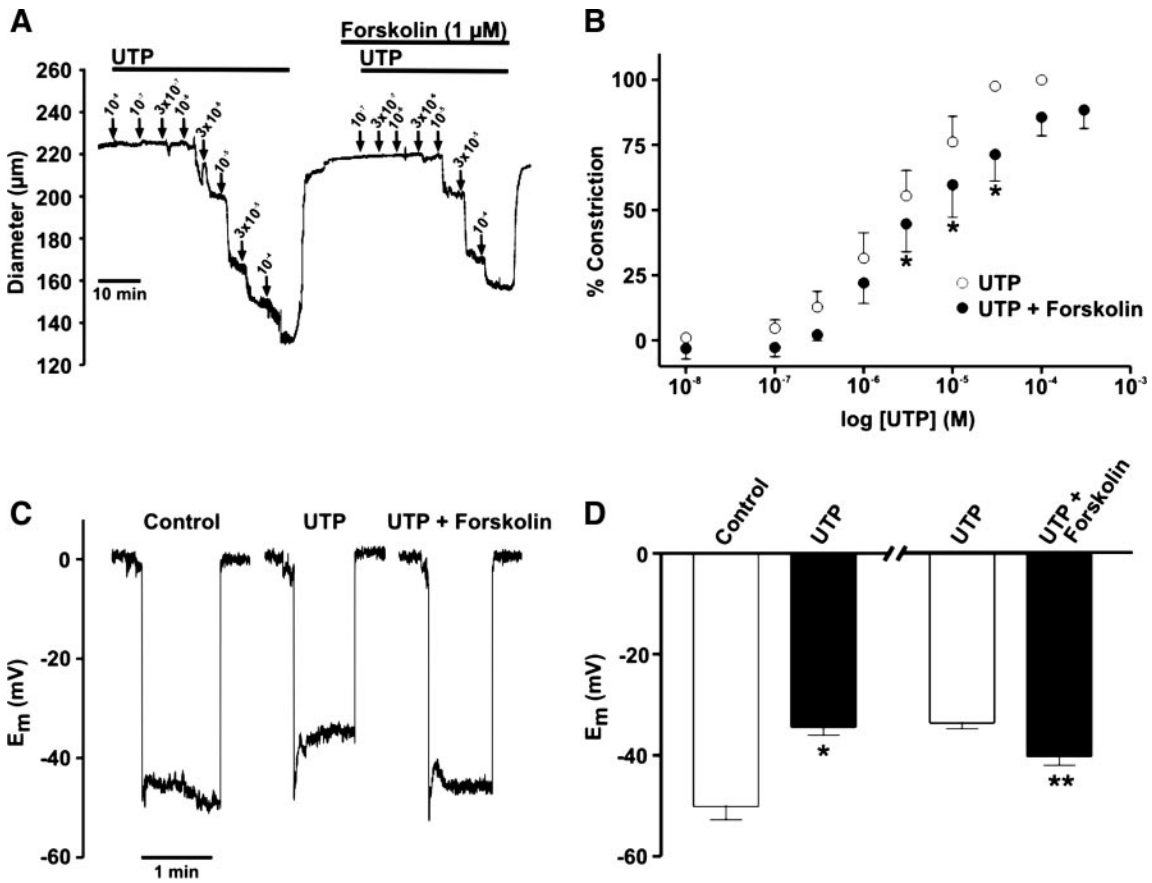

Fig. 6. PKA activation attenuates UTP-induced depolarization and constriction of cerebral arteries. *A*: representative trace of arterial constriction to an increasing concentration of UTP ± forskolin (1×10^{-6} M). *B*: summary data of the concentration-dependent effect of UTP ± forskolin on arterial diameter ($n = 6$). *C*: representative recordings of smooth muscle membrane potential (E_m) measured under control conditions and in the presence of UTP ± forskolin (1×10^{-6} M). *D*: summary data of the effect of UTP on E_m ($n = 8$) and effect of forskolin on UTP-induced depolarization ($n = 7$). *Statistical difference from control ($P \leq 0.05$). **Statistical difference from UTP-treated condition.

increasing at millimolar concentrations (26.5 ± 2.4, 34.0 ± 2.9, and 40.8 ± 3.8% at 1, 3, and 10 mM 4-AP, respectively). This study did not observe a voltage dependence to the 4-AP block as assessed at 0, +20, and +40 mV (data not shown).

Because RhoA is hypothesized to be a target of PKA and PKG, we sought to emphasize our previous finding that UTP suppresses the cerebral arterial K_{DR} current through a RhoA signaling pathway (18). As shown in Fig. 2*A*, a UTP concentration (3.0×10^{-5} M) that elicits a near-maximal constriction (18) suppressed the K_{DR} current, causing a 36.8 ± 4.1% inhibition at +40 mV (Fig. 2*A*, *right*). Consistent with the view that RhoA activity is a requisite for UTP modulation, C3 exoenzyme (10 mg/ml) eliminated current suppression (Fig. 2*B*). As evident in the summary data, there was no detectable change in the net current-voltage relationship after the addition of UTP to cells pretreated with C3 exoenzyme (Fig. 2*B*, *right*).

Regulation of K_{DR} current by PKA and PKG. Because past studies have indicated that PKA and PKG can phosphorylate and inactivate RhoA (6, 17, 19, 24, 26), this study tested whether activation of the PKA and PKG pathways can influence the ability of RhoA to suppress the K_{DR} current. As shown in Fig. 3, agents that directly (db-cAMP, 2×10^{-4} M) or indirectly (forskolin, 1×10^{-6} M) activate PKA did not alter the K_{DR} current under control conditions. They did, however, prevent UTP from suppressing this conductance. In a similar manner, agents that stimulate PKG either reduced (db-cGMP, from 36.8 ± 4.1% to 17.0 ± 3.3% at +40 mV) or abolished (SNP, 2×10^{-5} M) the UTP-induced suppression without effect on basal current (Fig. 4). Nitric oxide (1×10^{-7} M), the endogenous activator of guanylate cyclase, also prevented UTP from suppressing the K_{DR} current (Fig. 5).

Vasomotor and E_m measurements of intact cerebral arteries. The preceding findings indicate that PKA and PKG pathways should attenuate UTP-induced constriction by limiting the depolarization of vascular smooth muscle. To test this supposition, this study examined the ability of PKA and PKG activators to dilate and hyperpolarize UTP-constricted arteries. As evident in Fig. 6*A*, UTP induced a concentration-dependent constriction in cerebral arteries stripped of endothelium and maintained at low pressure (15 mmHg). Preincubation with 1×10^{-6} M forskolin attenuated the constrictor response, as evident by a significant rightward shift in vessel sensitivity to UTP (Fig. 6*B*). UTP (1×10^{-5} M) depolarized cerebral arteries from a resting E_m of −50.1 ± 2.6 to −34.4 ± 1.6 mV (Fig. 6, *C* and *D*). The addition of forskolin partially reversed this response, with arteries hyperpolarizing from −36.6 ± 1.2 to −43.8 ± 1.9 mV. Similar to PKA activation, activation of PKG by SNP attenuated UTP-induced constriction (Fig. 7, *A* and *B*). In addition, SNP partially

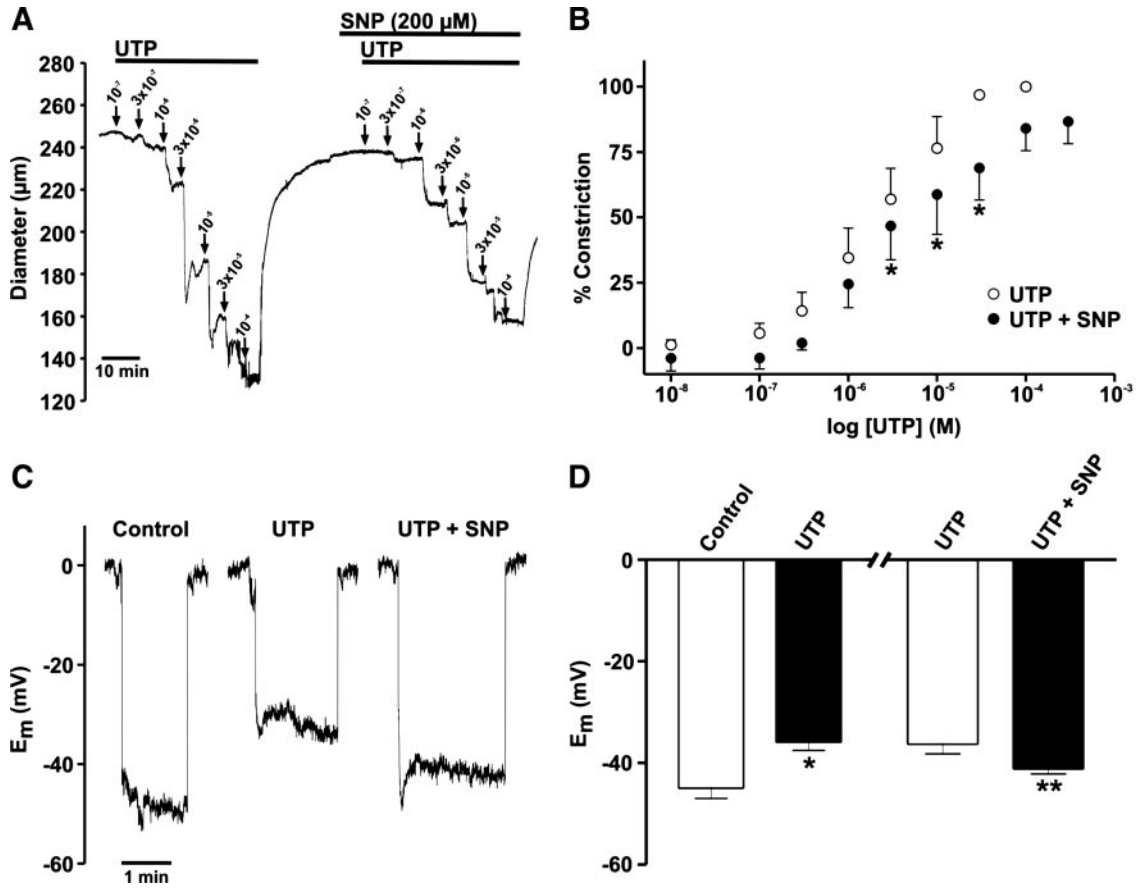

Fig. 7. PKG activation attenuates UTP-induced depolarization and constriction of cerebral arteries. *A*: representative trace of arterial constriction to an increasing concentration of UTP ± SNP (2×10^{-4} M). *B*: summary data of the concentration-dependent effect of UTP ± SNP on arterial diameter ($n = 6$). *C*: representative recordings of smooth muscle E_m measured under control conditions and in the presence of UTP ± SNP (2×10^{-4} M). *D*: summary data of the effect of UTP on E_m ($n = 7$) and the effect of SNP on UTP-induced depolarization ($n = 5$). *Statistical difference ($P \leq 0.05$). **Statistical difference from UTP-treated condition.

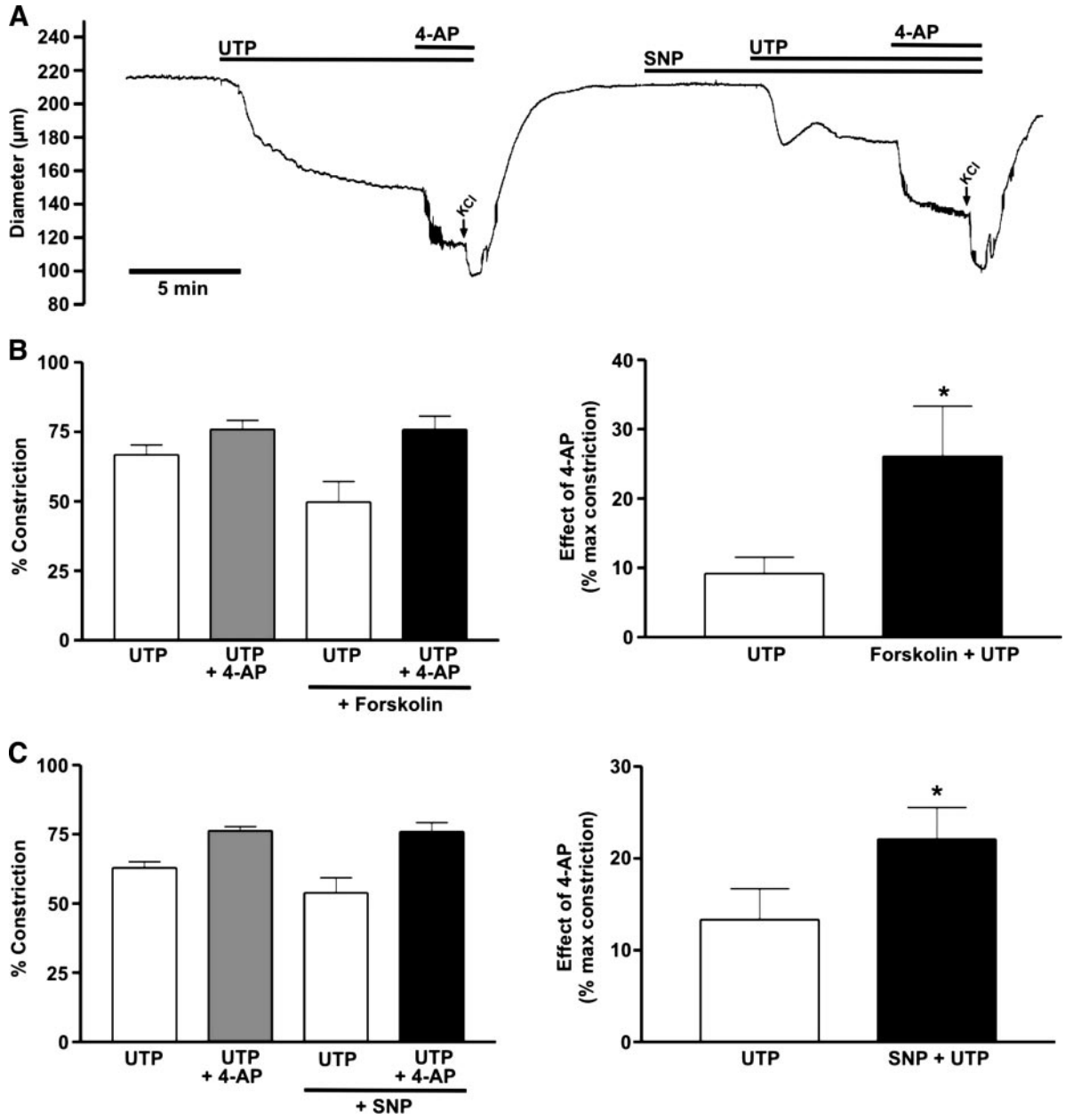

Fig. 8. PKA and PKG attenuate UTP-induced constriction by relieving inhibition of 4-AP-sensitive K_{DR} channels. *A*: representative trace of arterial diameter illustrating the effect of 5 mM 4-AP in the presence of UTP ± SNP (2×10^{-4} M). *B*: summary data of the effect of 4-AP on arterial diameter in the presence of UTP ± forskolin (*left*; $n = 6$). Effect of 4-AP in the presence of UTP ± forskolin is expressed as percentage of maximal constriction to 60 mM KCl (*right*). *C*: summary data of the effect of 4-AP on arterial diameter in the presence of UTP ± SNP (*left*; $n = 6$). Effect of 4-AP in the presence of UTP ± SNP is expressed as percentage of maximal constriction to 60 mM KCl (*right*). *Statistical difference ($P \leq 0.05$).

reversed UTP-induced depolarization, with E_m shifting from -36.3 ± 1.8 to -41.1 ± 1.0 mV (Fig. 7, *C* and *D*). These latter effects were induced with an SNP concentration 10-fold above that used in patch-clamp experiments. We attribute this discrepancy to the labile nature of this nitric oxide donor in bicarbonate-buffered solutions.

K_V channel modulation in intact cerebral arteries. In theory, the reversal of UTP-induced depolarization by PKA and PKG activators could result from a reduction in inward current and/or an increase in outward current. To more directly implicate the K_{DR} current, the constrictor response to 4-AP (5×10^{-3} M) was used as a functional assay of channel activity. As illustrated in Fig. 8*A*, cerebral arteries were first submaximally constricted to UTP. 4-AP was subsequently added to the superfusate to elicit a further constriction (Fig. 8, *B* and *C*, *left*), the magnitude of which should reflect the proportion of 4-AP-sensitive K_{DR} channels that remain active and not inhibited by UTP. The addition of forskolin or SNP to the superfusate attenuated UTP-induced constriction. More importantly, the 4-AP-induced constriction was noticeably larger in the presence of these indirect kinase activators, a result indicative of increased K_{DR} channel activity. This difference in the 4-AP response is emphasized in Fig. 8, *B* and *C*, *right*. Note that arteries exposed to both UTP and 4-AP were not maximally

constricted because the addition of 6×10^{-3} M extracellular K^+ elicited a further reduction in arterial diameter.

DISCUSSION

This study tested whether the PKA and PKG pathways prevent RhoA from inhibiting K_{DR} channels and thus limit the ability of vasoconstrictors to depolarize and constrict cerebral arteries. Electrophysiological experiments confirmed the presence of a cerebral arterial K_{DR} current that was suppressed by UTP through a RhoA-dependent mechanism. Without changing baseline channel activity, PKA and PKG activators attenuated the ability of UTP to inhibit the K_{DR} current. Pressure myography revealed that PKA and PKG activators hyperpolarized and dilated UTP-constricted arteries, a response that could be partly ascribed to increased activity of 4-AP-sensitive K_{DR} channels. Cumulatively, our findings indicate that PKA and PKG pathways can antagonize agonist-induced constriction and do so in part by limiting RhoA-mediated suppression of the K_{DR} current and the depolarization of cerebral resistance arteries.

K_{DR} current in cerebral arterial smooth muscle. Conventional whole cell patch-clamp electrophysiology was used to characterize the K_{DR} current in smooth muscle cells isolated from cerebral arteries. Similar to past studies from the cerebral and mesenteric circulation, the K_{DR} current displayed measurable activity at voltages positive to −40 mV and a voltage dependence of half-maximal activation of -0.56 ± 0.66 mV (Fig. 1). Although small in magnitude (~1–2 pA between −60 and −30 mV), the high-input resistance of vascular smooth muscle cells (5–20 GΩ) ensures that this current will play an important role in controlling E_m (5, 20). Our cerebral arterial K_{DR} currents displayed a sensitivity to 4-AP that is characteristic of vascular K_{DR}. In particular, a 15–20% reduction was observed at 4-AP concentrations (100–300 μM) thought to be specific for Kv1 channel block. As documented in the mesenteric artery (22), millimolar 4-AP was required to elicit a more substantial block (~34%) in cerebral arterial smooth muscle cells. The presence of a sizable 4-AP-resistant outward current indicates that a second population of K_{DR} channels may be present in cerebral and mesenteric arteries. Although their molecular composition is speculative, potential candidates include Kv2 (3) and Kv7 (21) subfamily members.

PKA and PKG pathways and the K_{DR} current. Past studies have shown that PKA and PKG can phosphorylate membrane-bound RhoA and inactive this key signaling protein (6, 17, 19, 24, 26). This process prevents RhoA from interacting with Rho kinase and is thus thought to relax smooth muscle by limiting Ca^{2+} sensitization (19, 24). From these observations and those indicating that active RhoA can modulate the 4-AP-sensitive K_{DR} current, we hypothesized that PKA and PKG pathways limit the ability of vasoconstrictors to inhibit the cerebral arterial K_{DR} current. In initiating this examination, we first confirmed that UTP suppresses the K_{DR} current and that this modulation was limited by C3 exoenzyme, an inhibitor of RhoA signaling (Fig. 2). As previously observed (18), current suppression peaked 15–20 min after UTP application, with the slow time course likely reflecting the cumulative effects of enzymatic isolation, room temperature recording conditions, and intracellular dialysis by the patch pipette. Stimulating PKA and PKG with either nonhydrolyzable cyclic nucleotide analogs or upstream cyclase activators effectively abolished K_{DR} current inhibition by UTP (Figs. 3–5). Intriguingly, basal K_{DR} current amplitude was unaffected by the presence of PKA and PKG activators, indicating that the underlying channels are not directly targeted for phosphorylation. These finding differ somewhat from rabbit portal vein and mesenteric artery, where K_{DR} currents were dramatically enhanced with PKA activation (1, 15). Whether these disparities reflect tissue-specific differences in kinase localization or perhaps unique K_{DR} channels with distinct regulatory capacities awaits further investigation. Although our electrophysiological examination indicates that PKA and PKG pathways regulate K_{DR} by attenuating the suppressive effects of Rho signaling, it does not directly implicate RhoA as the target of phosphorylation. Indeed, one could argue that it is other proteins within the Rho signaling cascade that are phosphorylated. Resolution of this issue awaits more in-depth biochemical and molecular analyses.

PKA and PKG pathways and cerebral arterial constriction. Ionic conductances such as the K_{DR} current actively control arterial tone by influencing E_m and, consequently, Ca^{2+} influx through voltage-gated L-type Ca^{2+} channels. From the preceding electrophysiological observations, one would predict that, in whole arteries, activation of the PKA and PKG pathways should attenuate agonist-induced depolarization and constriction. In keeping with this prediction, pressure myography revealed that forskolin and SNP limited UTP-induced vasoconstriction and partially reversed the associated depolarization (Figs. 6 and 7). Although supportive, these functional results do not directly implicate a role for 4-AP-sensitive K_{DR} channels in the hyperpolarizing response. Indeed, given the known sensitivity of smooth muscle K^+ conductances to PKA and PKG activators, one could rationalize that the preceding reversal simply arose from the activation of large-conductance Ca^{2+}-activated (2, 7, 33) or ATP-sensitive K^+ channels (13, 14, 27). To directly implicate a role for the 4-AP-sensitive K_{DR} current in the attenuation of agonist-induced depolarization, experiments were devised in which the constriction to millimolar 4-AP was used as a functional marker of channel activity. Consistent with a role for K_{DR} channels, 4-AP-induced responses were markedly greater in UTP-constricted vessels following forskolin and SNP application (Fig. 8). This increased 4-AP effect occurred despite the hyperpolarization

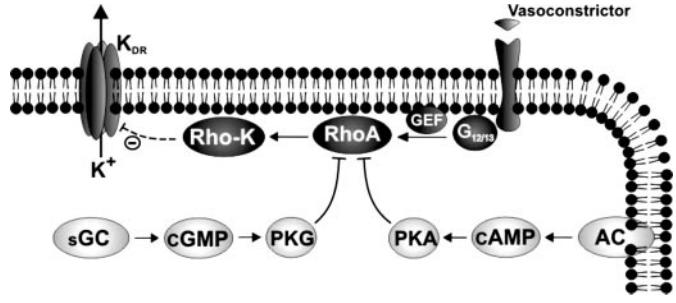

Fig. 9. A schematic of the proposed signaling mechanism by which PKA and PKG pathways prevent K_{DR} current suppression and limit constriction in cerebral arteries. Receptors coupled to $G_{12/13}$ activate RhoA/Rho kinase to suppress the K_{DR} current, thereby facilitating depolarization and constriction. We propose that the PKA and PKG pathways indirectly modulate K_{DR} by attenuating RhoA signaling, rather than by direct channel regulation. $G_{12/13}$, trimeric G protein; GEF, guanine nucleotide exchange factor; Rho-K, Rho kinase; AC, adenylate cyclase; sGC, soluble guanylate cyclase.

induced by forskolin and SNP (Fig. 7*C*), which reduces K_{DR} channel open probability and the chemical driving force for K^+. These functional observations provide compelling evidence that the PKA and PKG pathways can limit agonist-induced constriction and depolarization in part by attenuating RhoA signaling and the inhibition of 4-AP-sensitive K_{DR} channels (Fig. 9). It is important to consider that, although previous reports indicate that RhoA is likely targeted by PKA and PKG in smooth muscle (19, 24), our findings do not exclude the possibility that the cyclic nucleotides are directly regulating RhoA signaling in the cerebral circulation.

Physiological implications. A network of resistance arteries controls the magnitude and distribution of blood flow to cerebral tissue. Under dynamic conditions, tone within this network is regulated by multiple stimuli produced by changes in metabolism (11), neural activity (28), blood flow (8), and intravascular pressure (12, 16). Although cerebral tone varies under physiological conditions, dramatic alterations in perfusion would have a deleterious impact on cerebral function. It is within this context that one could suggest that the preceding mechanism of K_{DR} regulation ensures that vasoconstrictors do not overly constrict cerebral arteries and thus impair organ perfusion. The relative importance of this mechanism would, however, depend on the endogenous levels of PKA and PKG pathway activators. Agonists likely to be susceptible to such regulation include both pyrimidine and purine nucleotides (activators of P_{2Y} receptors) as well as thromboxane, all of which activate RhoA signaling (18, 25). Furthermore, it could be suggested that one means by which reduced endothelial nitric oxide synthase activity elevates cerebral tone during hypertension is through the loss of PKG signaling and its ability to impair K_{DR} inhibition and arterial depolarization.

In summary, this study demonstrated that activation of the PKA and PKG pathways prevents RhoA signaling from suppressing the cerebral arterial K_{DR} current. Importantly, this attenuation limited the ability of UTP to depolarize and constrict intact cerebral arteries. We propose that, under dynamic conditions, this newly described regulatory mechanism would prevent vasoconstrictors from overly constricting cerebral arteries and impairing tissue blood flow.

ACKNOWLEDGMENTS

The authors are grateful to Suzanne Brett Welsh and Randolph Corteling for assistance.

GRANTS

This work was supported by an operating grant from Canadian Institute for Health Research. D. G. Welsh is a senior scholar with the Alberta Heritage Foundation for Medical Research and holds a Canada Research Chair in vascular communication. K. D. Luykenaar is supported by a scholarship from the Heart and Stroke Foundation of Canada.

REFERENCES

1. **Aiello EA, Walsh MP, Cole WC.** Phosphorylation by protein kinase A enhances delayed rectifier K^+ current in rabbit vascular smooth muscle cells. *Am J Physiol Heart Circ Physiol* 268: H926–H934, 1995.
2. **Alioua A, Tanaka Y, Wallner M, Hofmann F, Ruth P, Meera P, Toro L.** The large conductance, voltage-dependent, and calcium-sensitive K^+ channel, Hslo, is a target of cGMP-dependent protein kinase phosphorylation in vivo. *J Biol Chem* 273: 32950–32956, 1998.
3. **Amberg GC, Santana LF.** Kv2 channels oppose myogenic constriction of rat cerebral arteries. *Am J Physiol Cell Physiol* 291: C348–C356, 2006.
4. **Bhattacharyya R, Wedegaertner PB.** Characterization of Gα13-dependent plasma membrane recruitment of p115RhoGEF. *Biochem J* 371: 709–720, 2003.
5. **Chen TT, Luykenaar KD, Walsh EJ, Walsh MP, Cole WC.** Key role of Kv1 channels in vasoregulation. *Circ Res* 99: 53–60, 2006.
6. **Ellerbroek SM, Wennerberg K, Burridge K.** Serine phosphorylation negatively regulates RhoA in vivo. *J Biol Chem* 278: 19023–19031, 2003.
7. **Fukao M, Mason HS, Britton FC, Kenyon JL, Horowitz B, Keef KD.** Cyclic GMP-dependent protein kinase activates cloned BKCa channels expressed in mammalian cells by direct phosphorylation at serine 1072. *J Biol Chem* 274: 10927–10935, 1999.
8. **Garcia-Roldan JL, Bevan JA.** Flow-induced constriction and dilation of cerebral resistance arteries. *Circ Res* 66: 1445–1448, 1990.
9. **Ghisdal P, Vandenberg G, Morel N.** Rho-dependent kinase is involved in agonist-activated calcium entry in rat arteries. *J Physiol* 551: 855–867, 2003.
10. **Gong MC, Fujihara H, Somlyo AV, Somlyo AP.** Translocation of rhoA associated with Ca^{2+} sensitization of smooth muscle. *J Biol Chem* 272: 10704–10709, 1997.
11. **Harder DR, Alkayed NJ, Lange AR, Gebremedhin D, Roman RJ.** Functional hyperemia in the brain: hypothesis for astrocyte-derived vasodilator metabolites. *Stroke* 29: 229–234, 1998.
12. **Harder DR, Gilbert R, Lombard JH.** Vascular muscle cell depolarization and activation in renal arteries on elevation of transmural pressure. *Am J Physiol Renal Fluid Electrolyte Physiol* 253: F778–F781, 1987.
13. **Hayabuchi Y, Dart C, Standen NB.** Evidence for involvement of A-kinase anchoring protein in activation of rat arterial K(ATP) channels by protein kinase A. *J Physiol* 536: 421–427, 2001.
14. **Hayabuchi Y, Davies NW, Standen NB.** Angiotensin II inhibits rat arterial KATP channels by inhibiting steady-state protein kinase A activity and activating protein kinase C. *J Physiol* 530: 193–205, 2001.
15. **Hayabuchi Y, Standen NB, Davies NW.** Angiotensin II inhibits and alters kinetics of voltage-gated K^+ channels of rat arterial smooth muscle. *Am J Physiol Heart Circ Physiol* 281: H2480–H2489, 2001.
16. **Knot HJ, Nelson MT.** Regulation of arterial diameter and wall $[Ca^{2+}]$ in cerebral arteries of rat by membrane potential and intravascular pressure. *J Physiol* 508: 199–209, 1998.
17. **Lang P, Gesbert F, Delespine-Carmagnat M, Stancou R, Pouchelet M, Bertoglio J.** Protein kinase A phosphorylation of RhoA mediates the morphological and functional effects of cyclic AMP in cytotoxic lymphocytes. *EMBO J* 15: 510–519, 1996.
18. **Luykenaar KD, Brett SE, Wu BN, Wiehler WB, Welsh DG.** Pyrimidine nucleotides suppress KDR currents and depolarize rat cerebral arteries by activating Rho kinase. *Am J Physiol Heart Circ Physiol* 286: H1088–H1100, 2004.
19. **Murthy KS, Zhou H, Grider JR, Makhlouf GM.** Inhibition of sustained smooth muscle contraction by PKA and PKG preferentially mediated by phosphorylation of RhoA. *Am J Physiol Gastrointest Liver Physiol* 284: G1006–G1016, 2003.
20. **Nelson MT, Quayle JM.** Physiological roles and properties of potassium channels in arterial smooth muscle. *Am J Physiol Cell Physiol* 268: C799–C822, 1995.
21. **Ohya S, Sergeant GP, Greenwood IA, Horowitz B.** Molecular variants of KCNQ channels expressed in murine portal vein myocytes: a role in delayed rectifier current. *Circ Res* 92: 1016–1023, 2003.
22. **Plane F, Johnson R, Kerr P, Wiehler W, Thorneloe K, Ishii K, Chen T, Cole W.** Heteromultimeric Kv1 channels contribute to myogenic control of arterial diameter. *Circ Res* 96: 216–224, 2005.
23. **Robertson BE, Nelson MT.** Aminopyridine inhibition and voltage dependence of K^+ currents in smooth muscle cells from cerebral arteries. *Am J Physiol Cell Physiol* 267: C1589–C1597, 1994.
24. **Sauzeau V, Le JH, Cario-Toumaniantz C, Smolenski A, Lohmann SM, Bertoglio J, Chardin P, Pacaud P, Loirand G.** Cyclic GMP-dependent protein kinase signaling pathway inhibits RhoA-induced Ca^{2+} sensitization of contraction in vascular smooth muscle. *J Biol Chem* 275: 21722–21729, 2000.
25. **Sauzeau V, Le Jeune H, Cario-Toumaniantz C, Vaillant N, Gadeau AP, Desgranges C, Scalbert E, Chardin P, Pacaud P, Loirand G.** P2Y(1), P2Y(2), P2Y(4), and P2Y(6) receptors are coupled to Rho and Rho kinase activation in vascular myocytes. *Am J Physiol Heart Circ Physiol* 278: H1751–H1761, 2000.

26. **Sawada N, Itoh H, Yamashita J, Doi K, Inoue M, Masatsugu K, Fukunaga Y, Sakaguchi S, Sone M, Yamahara K, Yurugi T, Nakao K.** cGMP-dependent protein kinase phosphorylates and inactivates RhoA. *Biochem Biophys Res Commun* 280: 798–805, 2001.
27. **Schubert R, Serebryakov VN, Mewes H, Hopp HH.** Iloprost dilates rat small arteries: role of K_{ATP}- and K_{Ca}-channel activation by cAMP-dependent protein kinase. *Am J Physiol Heart Circ Physiol* 272: H1147–H1156, 1997.
28. **Si ML, Lee TJ.** α7-Nicotinic acetylcholine receptors on cerebral perivascular sympathetic nerves mediate choline-induced nitrergic neurogenic vasodilation. *Circ Res* 91: 62–69, 2002.
29. **Somlyo AP, Somlyo AV.** Signal transduction and regulation in smooth muscle. *Nature* 372: 231–236, 1994.
30. **Somlyo AP, Somlyo AV.** Signal transduction by G-proteins, rho-kinase and protein phosphatase to smooth muscle and non-muscle myosin II. *J Physiol* 522: 177–185, 2000.
31. **Sward K, Mita M, Wilson DP, Deng JT, Susnjar M, Walsh MP.** The role of RhoA and Rho-associated kinase in vascular smooth muscle contraction. *Curr Hypertens Rep* 5: 66–72, 2003.
32. **Welsh DG, Nelson MT, Eckman DM, Brayden JE.** Swelling-activated cation channels mediate depolarization of rat cerebrovascular smooth muscle by hyposmolarity and intravascular pressure. *J Physiol* 527: 139–148, 2000.
33. **White RE, Kryman JP, El-Mowafy AM, Han G, Carrier GO.** cAMP-dependent vasodilators cross-activate the cGMP-dependent protein kinase to stimulate BK_{Ca} channel activity in coronary artery smooth muscle cells. *Circ Res* 86: 897–905, 2000.